THE JOURNAL OF BIOLOGICAL CHEMISTRY VOL. 283, NO. 16, pp. 10978–10991, April 18, 2008

Glycine Transporter Dimers

EVIDENCE FOR OCCURRENCE IN THE PLASMA MEMBRANE[*] [S]

Received for publication, January 24, 2008 Published, JBC Papers in Press, February 5, 2008, DOI 10.1074/jbc.M800622200

Ingo Bartholomäus[‡1], Laura Milan-Lobo[§], Annette Nicke[‡], Sébastien Dutertre[‡2], Hanne Hastrup[¶], Alok Jha[§], Ulrik Gether[¶], Harald H. Sitte[§3], Heinrich Betz[‡], and Volker Eulenburg[‡4]

From the [‡]Department of Neurochemistry, Max Planck Institute for Brain Research, Deutschordenstrasse 46, 60529 Frankfurt, Germany, [§]Center for Biomolecular Medicine and Pharmacology, Institute of Pharmacology, Medical University Vienna, Waehringerstrasse 13a, A-1090 Vienna, Austria, and [¶]Molecular Neuropharmacology Group and Center for Pharmacogenomics, Department of Pharmacology, The Panum Institute, University of Copenhagen, DK-2200 Copenhagen, Denmark

Different Na^+/Cl^--dependent neurotransmitter transporters of the SLC6a family have been shown to form dimers or oligomers in both intracellular compartments and at the cell surface. In contrast, the glycine transporters (GlyTs) GlyT1 and -2 have been reported to exist as monomers in the plasma membrane based on hydrodynamic and native gel electrophoretic studies. Here, we used cysteine substitution and oxidative cross-linking to show that of GlyT1 and GlyT2 also form dimeric complexes within the plasma membrane. GlyT oligomerization at the cell surface was confirmed for both GlyT1 and GlyT2 by fluorescence resonance energy transfer microscopy. Endoglycosidase treatment and surface biotinylation further revealed that complex-glycosylated GlyTs form dimers located at the cell surface. Furthermore, substitution of tryptophan 469 of GlyT2 by an arginine generated a transporter deficient in dimerization that was retained intracellulary. Based on these results and GlyT structures modeled by using the crystal structure of the bacterial homolog $LeuT_{Aa}$, as a template, residues located within the extracellular loop 3 and at the beginning of transmembrane domain 6 are proposed to contribute to the dimerization interface of GlyTs.

After presynaptic release and postsynaptic receptor activation, neurotransmitters have to be rapidly removed from the synaptic cleft in order to allow synaptic transmission to proceed with high spatial and temporal resolution. This is achieved by neurotransmitter transporters located in the plasma membrane of nerve terminals and adjacent glia cells. The family of Na^+/Cl^--dependent neurotransmitter transporters (SLC6a) includes transporters for γ-aminobutyric acid (GAT1 to -3),[5] glycine (GlyT1 and -2), dopamine (DAT), serotonin (SERT), and norephinephrine (NET) (1–3). All of these transporters display significant sequence similarity and share a common membrane topology with 12 transmembrane segments (TMs), a large second extracellular loop (EL2) connecting TM3 and TM4, and cytoplasmic N- and C-terminal regions. Although the functional unit of Na^+/Cl^--dependent transporters is thought to be a monomer, there is increasing evidence that these transporters form dimers or even higher oligomers within the plasma membrane (4). Oxidative treatment of the DAT produces dimers and tetramers due to intermolecular disulfide bond formation between two cysteine residues, Cys^{243} and Cys^{306}, located within TM4 and at the end of EL3, respectively (5, 6). Similarly, chemical cross-linking and co-isolation of differentially tagged transporter polypeptides has shown that the recombinant SERT forms oligomers in human embryonic kidney (HEK) 293 cells (7, 8). Furthermore, for the GAT, DAT, and SERT it has been shown that co-expression of the transporter polypeptides fused to cyan fluorescent protein (CFP) with the respective yellow fluorescent protein (YFP)-tagged protein results in a Förster resonance energy transfer (FRET) signal, suggesting that at least dimers of these transporters exist (9, 10). A possible oligomerization interface has been identified within TM2 of GAT1, where both the disruption of a leucine heptad motif and substitution of polar amino acid residues caused intracellular retention of the transporter and a loss of the FRET signal (11, 12). Also, x-ray crystallography of a bacterial ortholog of the SLC6a transporter family, $LeuT_{Aa}$, revealed that this transporter forms homodimers (13). Together, all of these data support the idea of Na^+/Cl^--dependent neurotransmitter transporters being oligomeric proteins.

There is, however, one reported exception from this rule, the glycine transporters GlyT1 and GlyT2 (14–16). These transporters mediate the uptake of the inhibitory neurotransmitter

* This work was supported by the Max-Planck-Gesellschaft, Deutsche Forschungsgemeinschaft (DFG) Grants SPP1172 and NI 592/3-2, Fonds der Chemischen Industrie, the Cluster of Excellence "Macromolecular Complexes" at the Goethe University Frankfurt (DFG Project EXC 115), and Austrian Science Fund Grants 17076 and 18076. The costs of publication of this article were defrayed in part by the payment of page charges. This article must therefore be hereby marked "*advertisement*" in accordance with 18 U.S.C. Section 1734 solely to indicate this fact.

[S] The on-line version of this article (available at http://www.jbc.org) contains supplemental Fig. S1.

[1] Present address: Max Planck Institute of Neurobiology, Am Klopferspitz 18, 82152 Martinsried, Germany.

[2] Recipient of a European Molecular Biology Organization postdoctoral fellowship.

[3] To whom correspondence may be addressed. Tel.: 43-1-4277-64123; Fax: 43-1-4277-9641; E-mail: harald.sitte@meduniwien.ac.at.

[4] To whom correspondence may be addressed. Tel.: 49-69-96769-317; Fax: 49-69-96769-441; E-mail: eulenburg@mpih-frankfurt.mpg.de.

[5] The abbreviations used are: GAT, γ-aminobutyric acid transporter; CFP, cyan fluorescent protein; CRFR1, corticotropine-releasing factor receptor 1; CuP, copper *o*-phenanthroline; DAT, dopamine transporter; EL, extracellular loop; FRET, fluorescence resonance energy transfer; $FRET_c$, corrected FRET; GlyT, glycine transporter; HEK 293T cells, human embryonic kidney 293T cells; His, heptahistidyl; NET, norepinephrine transporter; PBS, phosphate-buffered saline; SERT, serotonin transporter; TM, transmembrane domain; YFP, yellow fluorescent protein; WT, wild type; NTA, nitrilotriacetic acid.

glycine from the extracellular space into glial cells (GlyT1) and glycinergic neurons (GlyT2), respectively (3). Studies on GlyT-deficient mice have shown that, after birth, GlyT1 is essential for removing glycine from postsynaptic glycine receptors (17), whereas GlyT2 is required for the reuptake of glycine into the presynaptic terminal (18). Additionally, GlyT1 has been shown to be involved in the regulation of glutamatergic neurotransmission by controlling the occupancy of the glycine binding site of the *N*-methyl-D-aspartate subtype of glutamate receptors (19–21). Evidence for a predominantly monomeric state of these transporters came from two independent studies that failed to detect oligomeric GlyTs within the plasma membrane. Both hydrodynamic analysis of GlyT1 solubilized from rat spinal cord (15) and affinity purification of surface-labeled recombinant GlyT1 and GlyT2 followed by blue native PAGE (14) provided evidence for GlyTs being monomers at the cell surface. Dimers and oligomers were only detected in intracellular membranes and suggested to represent overexpression artifacts (14). Here, we used a combination of mutagenesis and cysteine-mediated cross-linking as well as FRET analysis in living cells to reexamine whether GlyTs form oligomers. Our data indicate that these transporters are dimers not only in intracellular compartments but also in the plasma membrane of HEK 293T cells.

EXPERIMENTAL PROCEDURES

Homology Modeling—The crystal structure of the bacterial leucine transporter $LeuT_{Aa}$ (Protein Data Bank code 2A65) was used as a template to build a homology model of GlyT2. To this end, the amino acid sequence of GlyT2 (accession no. Q761V0) (22) was truncated at its N and C termini (residues 1–192 and 747–799, respectively), and the large EL2 (residues 313–364) was deleted. The remaining sequence was aligned with $LeuT_{Aa}$ according to Yamashita *et al.* (13). Three-dimensional models (10 structures) of GlyT1 and GlyT2 were built from the aligned sequences on a Silicon Graphics Octane R12000 work station using the MODELLER program (23). The models resulting in the lowest root mean square deviation as compared with the original $LeuT_{Aa}$ structure were retained for analysis without further refinement. Dimers of GlyT2 were created by juxtaposing two transporter molecules using Thr^{464} as an anchoring point. Figures were generated using PyMOL software (Delano Scientific, Palo Alto, CA).

cDNA Constructs and Heterologous Expression—An expression construct for the human GlyT1c was kindly provided by Dr. Katherine Fisher (Groton Laboratories, Pfizer, NY). The GlyT2 cDNA was isolated from mouse brain stem mRNA using standard cloning techniques. N-terminal heptahistidyl (His), FLAG, and Myc tags were added by PCR-based mutagenesis. After subcloning into the pcDNA3.1$^+$ vector (Invitrogen), the respective substitutions were introduced by using the QuikChange site-directed mutagenesis kit (Stratagene, La Jolla, CA). For fluorescence analysis, the coding regions of GlyT1 and GlyT2 were subcloned by PCR into pECFP-C1 or pEYFP-C1 (Clontech-Takara Bio Europe, Saint-Germain-en-Laye, France) to create CFP- or YFP-tagged GlyT1 or GlyT2, respectively. All constructs were verified by sequencing, and all surface-expressed transporters were shown to be functional upon heterologous expression in HEK 293T cells as revealed by [^{3}H]glycine uptake measurements (data not shown). An expression construct for the human DAT (24) was kindly provided by Dr. Marc G. Caron (Duke University, Durham, NC), and a membrane-bound form of YFP (25) was kindly provided by Viacheslav Nikolaev (University of Würzburg, Germany).

HEK 293T cells were grown in modified Eagle's medium supplemented with glutamine (2 mM), 10% (v/v) fetal calf serum, penicillin (50 units/ml), streptomycin (50 μg/ml), and 50 μM β-mercaptoethanol (all reagents from Invitrogen) at 37 °C in a humidified 5% CO_2 atmosphere. Cells were seeded on the day prior to transfection into 6-well plates, and transfection was performed at 70–85% confluence using the Polyfect transfection reagent (Qiagen, Hilden, Germany) according to the manufacturer's protocol. For GlyT1 expression, GripTite 293 cell lines (Invitrogen) stably expressing GlyT1, $GlyT1^{L343C}$, and $GlyT1^{C116A;L343C}$ were generated and seeded 48 h before the experiment.

Oxidative Cross-linking—Cross-linking experiments were performed 48–72 h after transfection. Adherent cells were washed twice with phosphate-buffered saline (PBS) or HEPES buffered salt solution (130 mM NaCl, 1.3 mM KCl, 1.2 mM $MgSO_4$, 1.2 mM KH_2PO_4, 2 mM $CaCl_2$, 10 mM glucose, 10 mM NaOH/HEPES, pH 7.4) and incubated with 0.1–0.5 mM $CuSO_4$ and 0.8–2 mM *o*-phenanthroline (CuP) in PBS or HEPES buffered salt solution for 10 min at room temperature. The reaction was stopped by removal of the reagent and incubation of the cells with 10 mM *N*-ethylmaleimide in PBS for 15–20 min.

Western Blotting—Cells were lysed at 4 °C in lysis buffer containing 150 mM NaCl, 5 mM EDTA, 1% (v/v) Triton X-100, 0.25% (w/v) desoxycholate, 0.1% (w/v) SDS, 1 mM Pefabloc SC (Roche Applied Science), and 50 mM HEPES/Tris, pH 7.4. After centrifugation for 15 min at 16,000 × *g*, the protein content in the supernatant was determined using the Bio-Rad Protein assay (Bio-Rad, Munich, Germany), and 10 μg of supernatant protein were mixed with the appropriate volume of 4× nonreducing loading buffer (Invitrogen) prior to separation by SDS-PAGE on 3–8% Tris acetate gels (Invitrogen). Proteins were transferred to either nitrocellulose (Whatman, Dassel, Germany) or polyvinylidene fluoride (Amersham Biosciences) membranes. The membranes were blocked in Tris-buffered saline supplemented with 0.1% (w/v) Tween 20 and 5% (w/v) nonfat milk powder for at least 30 min prior to a ≥30-min incubation with primary antibodies directed against either the N terminus of GlyT2 (polyclonal rabbit) (18), DAT (polyclonal rabbit, Chemicon, Temecula, CA), the Myc epitope (polyclonal rabbit, Abcam, Cambridge, UK) (all diluted 1:2000 in blocking buffer), or the FLAG epitope (monoclonal mouse; Sigma; 4 μg/ml). After washing with Tris-buffered saline containing 0.5% (w/v) Tween 20, membranes were incubated with horseradish peroxidase-conjugated goat anti-rabbit antibodies (Invitrogen) and detected with the SuperSignal kit (Pierce).

Affinity Purification of His-tagged GlyT2—HEK 293T cells were transfected with the indicated constructs and, 48 h later, lysed in 100 mM sodium phosphate buffer, pH 8.0, containing 0.2% (w/v) dodecylmaltoside and 1 mM Pefabloc SC. The lysates were centrifuged at 16,000 × *g* for 15 min, and 190 μg of supernatant protein were incubated under continuous agitation with

Ni^{2+}-NTA-agarose beads (Qiagen, Hilden, Germany) in the aforementioned lysis buffer supplemented with 10 mM imidazole for 1 h at 4 °C. After washing with lysis buffer containing 30 mM imidazole and 0.075% (w/v) dodecylmaltoside, agarose-bound proteins were eluted with 2× SDS loading buffer (Invitrogen) for 10 min at 25 °C.

Functional Characterization of GlyT2—His-$GlyT2^{WT}$ or His-$GlyT2^{T464C}$ was expressed in *Xenopus laevis* oocytes as described previously (14). Glycine (30 μM)-induced currents were monitored using the two-electrode voltage clamp technique as described previously (26). The oocytes were treated with 5 mM CuP for 15 min, and glycine-induced currents were measured again. To analyze the efficacy of CuP-induced cross-linking, His-tagged proteins were isolated from detergent extracts of these oocytes as described (14) and subjected to Western blot analysis. Dimers of 200 kDa were only seen after CuP treatment of His-$GlyT2^{T464C}$ but not of untreated or His-$GlyT2^{WT}$-expressing cells (data not shown).

Surface Biotinylation—Surface biotinylation of transfected HEK 293T cells with 1 mM NHS-SS-biotin (Pierce) was performed essentially as described (27). After biotinylation, cell lysates (50 μg of protein) were incubated with streptavidin-agarose beads (60 μl; Pierce) for 3 h at 4 °C. The beads were then washed three times with lysis buffer, and bound biotinylated proteins were eluted by a 30-min incubation at 4 °C with 30 μl of 1× loading buffer (Invitrogen) supplemented with 0.6 mM dithiothreitol. Aliquots of the lysates (15 μg of protein) and biotinylated fractions (30 μl) were then analyzed by SDS-PAGE and Western blotting.

Fluorescence Resonance Energy Transfer—FRET signals (28) were measured with an epifluorescence microscope (Carl Zeiss Axiovert 200) using the "three-filter method" according to Xia and Liu (29). Images were taken from HEK 293 cells maintained and transfected as described previously (30) using a ×63 oil objective and a LUDL filter wheel that allows for rapid exchange of filters. The system was equipped with the following fluorescence filters: CFP filter (I_{CFP}; excitation = 436 nm, dichroism = 455 nm, emission = 480 nm), YFP filter (I_{YFP}; excitation = 500 nm, dichroism = 515 nm, emission = 535 nm), and FRET filter (I_{FRET}; excitation = 436 nm, dichroism = 455 nm, emission = 535 nm). The acquisition of the images was done with MetaMorph version 4.6. (Molecular Devices Corp., Downingtown, PA). Background fluorescence was subtracted from all images, and fluorescence intensity was measured at the plasma membrane and in cytosolic regions in all images. To calculate a normalized FRET signal (N_{FRET}), we used the following equation,

$$N_{FRET} = \frac{I_{FRET} - a \times I_{YFP} - b \times I_{CFP}}{\sqrt{I_{YFP} \times I_{CFP}}} \qquad \text{(Eq. 1)}$$

where a and b represent the bleed-through values for YFP and CFP. All N_{FRET} values are expressed as means ± S.E. Corrected FRET ($FRET_c$) images were obtained according to Ref. 31. Briefly, after background subtraction from all three images, CFP and YFP images were multiplied with their corresponding bleed-through value. The following equation was used for the calculation of $FRET_c$ images, $FRET_c = FRET - (b \times CFP) - (a \times YFP)$.

Confocal Microscopy—GlyT cell surface expression was visualized by confocal microscopy using a Zeiss Axiovert 200-LSM 510 confocal microscope (argon laser, 30 milliwatts; helium/neon laser, 1 milliwatt) equipped with an oil immersion objective (Zeiss Plan-Neofluar ×40/1.3). In brief, HEK 293 cells transfected with the indicated construct were seeded onto glass coverslips and examined 1 day later. In co-expression experiments, fluorescent protein-tagged constructs were detected with a band pass filter (475–525 nm) using the 458-nm (for CFP, at 30–45% input power) or 488 nm (for YFP, at 8–10% input power) laser lines. Plasma membranes were visualized after the addition of 20 μl of trypan blue (0.05% (w/v) in PBS) at an excitation wavelength of 543 nm with a long pass filter (585 nm). CFP and trypan blue images were captured sequentially, and overlay images were produced with Zeiss imaging software as described (32).

RESULTS

For the DAT, residue Cys^{306}, located at the end of EL3 between TM5 and TM6, has been shown to be essential for intermolecular disulfide bond formation upon oxidative treatment (5). Sequence comparison revealed that in the GlyTs, leucine and threonine residues are found at the homologous positions (Leu^{343} in GlyT1c and Thr^{464} in GlyT2; Fig. 1*A*). To assess whether these residues reside at the surfaces of the respective transporter proteins and might be close to a possible dimerization interface, we generated a model of GlyT2 by using the crystal structure of $LeuT_{Aa}$ as a template (13). Regions that did not display significant homology to the $LeuT_{Aa}$ protein, like the intracellular N and C termini and the large EL2 between TM3 and TM4, were deleted from the GlyT2 sequence to optimize sequence alignment. The resulting GlyT2 model showed a root mean square deviation of 3.62 Å from the $LeuT_{Aa}$ structure when 498 of 504 pairwise Cα atoms were aligned (root mean square deviation of 1.157 Å for 398 Cα atoms). In this model, the side chain of Thr^{464} was located on the surface of the transporter above the helix formed by TM11 (Fig. 1, *B* and *C*). Thus, Thr^{464} might be close to a possible dimerization interface. Apposition of two monomers at this interface created a GlyT2 dimer, in which the two Thr^{464} residues are in close proximity (Fig. 1, *B–E*). This dimeric model suggests that, in addition to interactions between the EL3 regions of the monomers, side chains of TM11 could contribute to dimer stabilization. Likewise, in a similar model of GlyT1, Leu^{343}, the amino acid residue corresponding to Thr^{464} in GlyT2 and Cys^{306} in DAT, is predicted to be localized at the surface of the transporter protein (data not shown).

To establish whether Thr^{464} is indeed located at a dimerization interface of GlyT2, we replaced this residue by a cysteine in order to examine whether GlyT2 oligomers can be stabilized by intermolecular disulfide cross-linking, as reported for the DAT (5). As controls, we generated two GlyT2 expression constructs, in which residues Lys^{462} and Thr^{557} were substituted by cysteines. According to our model, both residues are unlikely to face the proposed dimerization interface (Fig. 1, *B–E*). HEK 293T cells were transfected with these three cysteine-substituted GlyT2 constructs and analyzed for [^{3}H]glycine uptake activity and subcellular localization of GlyT2 immunoreactiv-

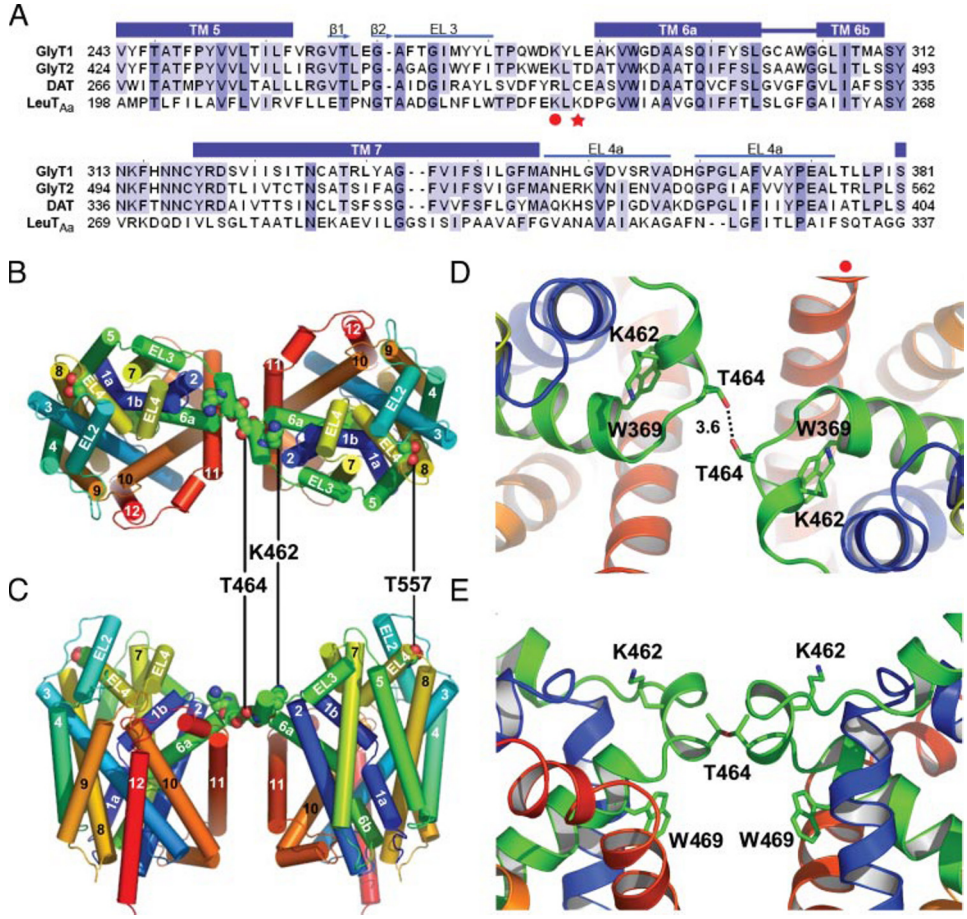

FIGURE 1. **Model of the structure of GlyT2.** *A*, alignment of partial amino acid sequences of GlyT1, GlyT2, DAT, and $LeuT_{Aa}$. *B–E*, homology model of GlyT2 based on the crystal structure of $LeuT_{Aa}$. *B* and *C*, the putative GlyT2 dimer is depicted from the extracellular side (*B*) and within the plane of the membrane (*C*). Helices (*cylinders*) are *numbered* following the $LeuT_{Aa}$ nomenclature (13). *D* and *E*, close-up views of the dimer interface shown in *B* and *C*. Residues substituted in this study are indicated.

ity. This did not reveal any significant differences as compared with wild-type GlyT2 ($GlyT2^{WT}$; data not shown). Western blot analysis of detergent extracts prepared from the transfected cells confirmed that the mutant transporters were expressed in amounts comparable with that obtained with the $GlyT2^{WT}$ cDNA (Fig. 2*C*). Two bands of 65 and 90 kDa, which represent the core-glycosylated and fully glycosylated transporter forms (33), were seen with all three mutant proteins. An additional band at about 155 kDa present in variable amounts presumably corresponded to SDS-resistant dimers of immature transporter polypeptides (14). Together, these data indicate that none of the cysteine substitutions introduced affected the expression, function, or plasma membrane insertion of GlyT2 in HEK 293T cells.

The $GlyT2^{T464C}$ Mutant Efficiently Forms Dimers—To determine whether position Thr^{464} is close to a potential dimerization interface of GlyT2, HEK 293T cells transiently expressing $GlyT2^{WT}$, the $GlyT2^{T464C}$ mutant, or, as a control, DAT^{WT} were treated with the oxidizing agent CuP, followed by detergent extraction, nonreducing SDS-PAGE, and Western blot analysis. With DAT^{WT}-expressing cells, CuP treatment resulted in the appearance of a distinct band at 170 kDa in addition to immunoreactive bands at 85 and 57 kDa (Fig. 2*A*), which represent the mature and immature monomeric forms of this transporter (5). The 170 kDa band corresponds in size to the previously described DAT^{WT} dimer (5), thereby confirming a close proximity of the Cys^{306} residues at the dimer interface. Consistent with previous findings (5), the formation of DAT dimers by CuP was completely abolished when Cys^{306} was replaced by an alanine (DAT^{C306A}; Fig. 2*A*).

In contrast to these results obtained with DAT^{WT}, CuP treatment of cells expressing $GlyT2^{WT}$ did not result in the formation of SDS-resistant GlyT2 oligomers (Fig. 2*B*, *left*). However, CuP treatment of $GlyT2^{T464C}$-expressing cells generated a major GlyT2-immunoreactive adduct of 200 kDa. This was accompanied by a strong decrease in the intensity of the 90 kDa band, which represents the fully glycosylated GlyT2 monomer (Fig. 2*B*, *left*). These results are consistent with $GlyT2^{T464C}$ forming a dimer that is cross-linked upon oxidative treatment. To exclude the possibility that this 200-kDa adduct represents an unspecific aggregate induced by CuP treatment, detergent extracts from CuP-treated cells expressing $GlyT2^{T464C}$ were supplemented with β-mercaptoethanol. This reducing treatment resulted in a strong reduction of the 200 kDa band and an increase in the intensity of the mature monomer band at 90 kDa indicative of cleavage of the disulfide cross-link (Fig. 2*B*, *right*). Notably, in contrast to what was found with $GlyT2^{T464C}$, CuP treatment of $GlyT2^{T557C}$- or $GlyT2^{K462C}$-expressing cells failed to produce the 200-kDa GlyT2 immunoreactive adduct (Fig. 2*C*). Thus, disulfide-mediated cross-linking of the $GlyT2^{T464C}$ mutant is position-specific.

The functional consequences of CuP cross-linking were analyzed by measuring glycine-induced currents by two-electrode voltage clamp in *Xenopus* oocytes expressing His-$GlyT2^{WT}$ or His-$GlyT2^{T464C}$ before and after treatment with CuP. Application of 30 μM glycine induced currents of 76 ± 8 pA for $GlyT2^{WT}$ and 39 ± 5 pA for $GlyT2^{T464C}$ ($n = 6$). The smaller current monitored for the $GlyT2^{T464C}$ mutant most likely reflects a slightly reduced expression also seen in Western blots prepared from detergent extracts from the oocytes (data not shown). After treatment with CuP, the currents recorded from the same oocytes were not significantly reduced as compared with the currents measured before cross-linking (reduction of 18 ± 13% for His-$GlyT2^{WT}$ and of 15 ± 12% for His-$GlyT2^{T464C}$, as compared with the untreated controls; $p \geq 0.5$). Similar to what was seen in HEK 293T cells, treatment of His-$GlyT2^{T464C}$ but not His-$GlyT2^{WT}$-expressing oocytes with

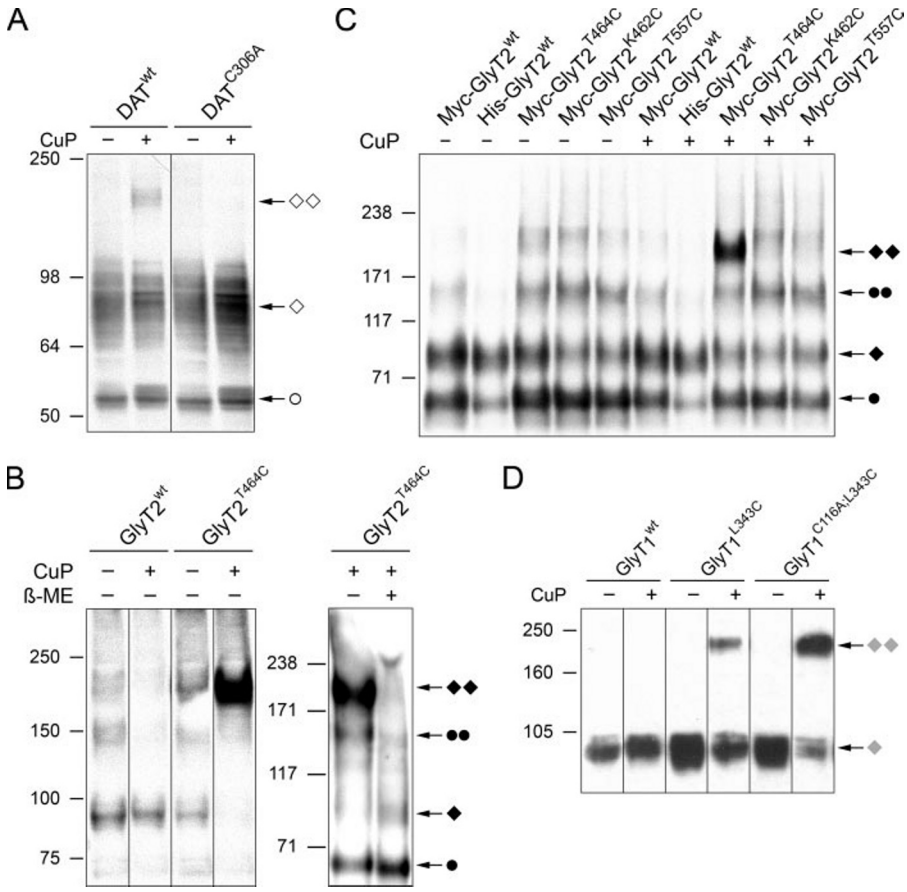

FIGURE 2. **Oxidative cross-linking of cysteine-substituted GlyTs.** *A*, Western blot of detergent extracts of HEK 293T cells expressing DAT^{WT} or DAT^{C306A}. The cells were treated with PBS (−) or CuP (+), prior to SDS-PAGE and immunoblotting with a DAT-specific antibody. Bands assigned to the immature monomer (○), the mature monomer (◇), and its dimer (◇ ◇) are indicated. *B* (*left*), HEK 293T cells were transfected with $GlyT2^{WT}$ or $GlyT2^{T464C}$ and treated with CuP (+), or PBS (−), prior to detergent extraction and Western blot analysis with a GlyT2-specific antibody. *Right*, detergent extracts from CuP-treated cells expressing $GlyT2^{T464C}$ were supplemented with β-mercaptoethanol (100 mM) or left untreated, prior to Western blot analysis with a GlyT2-specific antibody. *C*, Western blot of detergent extracts prepared from HEK 293T cells expressing Myc- or His-tagged $GlyT2^{WT}$ and the Myc-$GlyT2^{T464C}$, Myc-$GlyT^{K462C}$, or Myc-$GlyT2^{T557C}$ mutants. Prior to detergent extraction, cells were treated with CuP (+) or PBS (−), as indicated. *D*, GripTite 293 cells expressing FLAG-tagged GlyT1, $GlyT1^{L343C}$, or $GlyT1^{C116A/L343C}$ were treated with CuP (+) or PBS (−), prior to detergent extraction and Western blot analysis with an anti-FLAG antibody. Note that both GlyTs formed adducts of higher molecular weight upon treatment with CuP only when cysteine-substituted. Different transporter forms are indicated: ●, immature monomer; ◆, mature monomer; ●●, immature dimer; ◆ ◆, mature dimer. *Filled symbols*, GlyT2; *shaded symbols*, GlyT1.

CuP resulted in the appearance of a prominent GlyT2-immunoreactive band at 200 kDa (data not shown). Together, these results are consistent with cross-linking of GlyT2 dimers by CuP treatment not interfering with transporter function.

Very similar findings were also obtained with GlyT1. CuP treatment of $GlyT1^{WT}$ stably expressing cells did not result in the appearance of a immunoreactive band of higher molecular weight. However, treatment of a $GlyT1^{L343C}$-expressing cell line produced a prominent immunoreactive band at 190 kDa. To exclude the possibility that this dimer formation might involve oxidation of the extracellular cysteine Cys^{116}, we repeated this experiment with a $GlyT1^{C116A/L343C}$ double mutant. Again efficient formation of the 190-kDa adduct was seen. Thus, Cys^{116} is not involved in oxidative cross-linking (Fig. 2*D*). The slight increase in cross-linking efficacy seen in cells expressing the $GlyT1^{C116A/L343C}$ double mutant most likely reflects differences in expression levels between the stable cell lines used. Taken together, these data demonstrate that the apparent molecular weight of both GlyTs increase by a factor of about 2 upon treatment with CuP when residues homologous to Cys^{306} within the DAT are substituted by cysteines.

Transporters Cross-linked by CuP Are Found in the Plasma Membrane—To determine the subcellular localization of the cross-linked $GlyT2^{T464C}$ protein, we first examined its glycosylation status. Previous studies have shown that complex-glycosylated GlyTs are predominantly localized in the plasma membrane, whereas immature core-glycosylated or nonglycosylated transporter forms are retained in intracellular compartments (34, 35). When detergent extracts prepared from CuP-treated HEK 293T cells expressing $GlyT2^{WT}$ or the $GlyT2^{T464C}$ mutant were incubated with endoglycosidase H, an enzyme that selectively removes core glycosylations from proteins, the apparent molecular mass of the band at 90 kDa did not change, but that of the immunoreactive 65 kDa band was reduced to 60 kDa (Fig. 3*A*). This confirms that the 65-kDa polypeptide represents the core-glycosylated form of GlyT2 (35). In addition, treatment with endoglycosidase H reduced the molecular mass of the 155 kDa immunoreactive band to about 140 kDa, indicating that this GlyT2 complex is derived from immature, and thus presumably intracellularly localized, GlyT2 protein (14). In contrast, the immunoreactive band at 200 kDa generated upon CuP treatment of $GlyT2^{T464C}$ was insensitive to treatment with endoglycosidase H (Fig. 3*A*). Thus, this cross-linked GlyT2 adduct did not contain core-glycosylated proteins. Incubation of the lysates from these cells with peptide:*N*-glycosidase F reduced the apparent molecular masses of all major immunoreactive bands to 140 and 60 kDa, respectively (Fig. 3*A*). Together, these data support our conclusion that the bands at 155 and 200 kDa represent GlyT2 dimers that differ in their glycosylation status.

To directly assess which of the GlyT2 forms detected above reside in the plasma membrane, we performed cell surface biotinylation experiments with CuP-treated cells expressing either $GlyT2^{WT}$ or $GlyT2^{T464C}$ (Fig. 3*B*). Subsequently, the biotinylated surface proteins were separated from nonbiotinylated intracellular proteins by using a streptavidin-agarose pull-

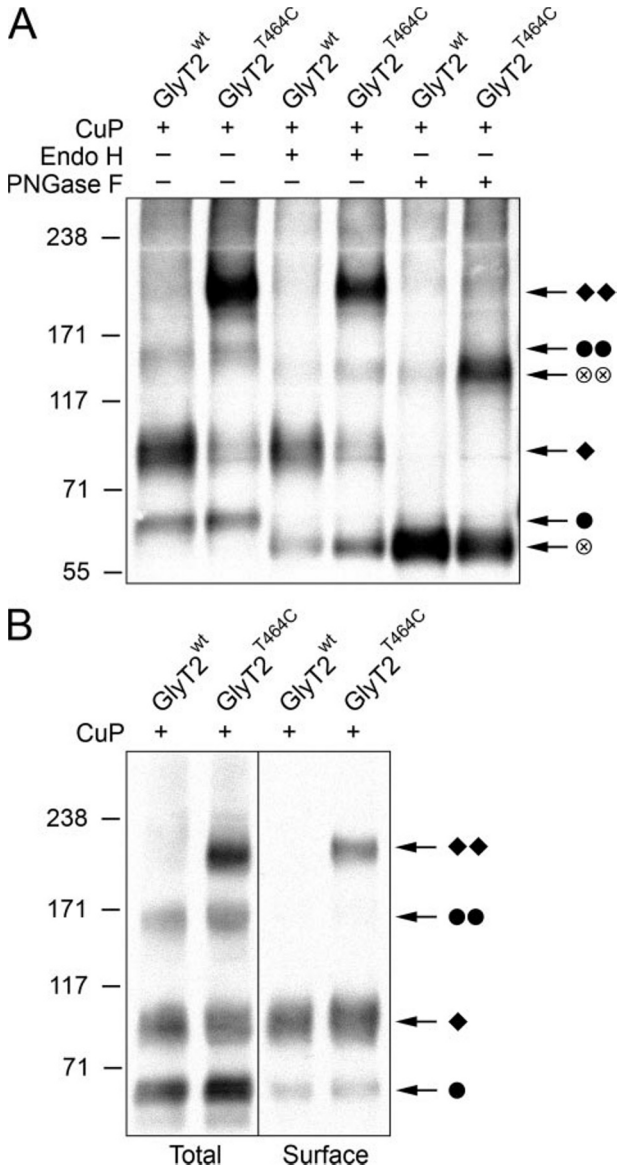

FIGURE 3. **The CuP-induced GlyT2 adduct is complex-glycosylated and localized at the cell surface.** *A*, detergent extracts of CuP (+)-treated HEK 293T cells transfected with His-GlyT2^{WT} or His-GlyT2^{T464C} were incubated with endoglycosidase H (*Endo H*) or peptide:*N*-glycosidase F (*PNGase F*), as indicated, and analyzed by Western blotting using a GlyT2-specific antibody. *B*, HEK 293T cells transfected with His-GlyT2^{WT} or His-GlyT2^{T464C} were treated with CuP (+), washed, and subjected to surface biotinylation. Aliquots of the detergent extracts prepared from these cells (*total*) as well as the eluates from the streptavidin-agarose beads containing the biotinylated proteins (surface) were analyzed by Western blotting analysis with GlyT2-specific antibodies. Different transporter forms are indicated as follows. ●, immature monomer; ⊗, deglycosylated monomer; ◆, mature monomer; ●●, immature dimer; ⊗⊗, deglycosylated dimer; ◆◆, mature dimer.

down approach. Western blot analysis of the bound biotinylated protein fraction revealed that the bands at 90 and 200 kDa representing mature monomeric transporter and the cross-linked putative GlyT2^{T464C} homodimer, respectively, were enriched within the surface fraction. Thus, a major fraction of the CuP-cross-linked GlyT2^{T464C} protein is localized in the plasma membrane. The apparently increased 90 kDa/200 kDa ratio seen in the GlyT2^{T464C} eluate might reflect cleavage of some of the cross-linked dimer during affinity isolation, due to inclusion of a low concentration of dithiothreitol being required for efficient elution from the streptavidin-agarose beads (see "Experimental Procedures").

GlyT Oligomerization Monitored by FRET—To further corroborate the existence of GlyT dimers in the plasma membrane by an independent technique, we employed FRET microscopy (28) using the three-filter method according to Xia and Liu (29) that allows us to quantitatively monitor protein oligomerization. Visualization of protein oligomerization in intact cells was achieved by the method of Sorkin *et al.* (31), which generates FRET$_c$ images. Cytosolic proteins known to lack or only spuriously form oligomeric complexes, enhanced CFP and enhanced YFP, were used as background controls. To provide a reference for membrane protein oligomerization, we co-expressed CFP- and YFP-tagged versions of the human DAT (C-DAT and Y-DAT, respectively), which has been shown to homo-oligomerize by both FRET microscopy and biochemical approaches (5, 10, 36). In addition, we used SERT tagged with CFP and YFP on its cytoplasmic N and C termini, respectively (C-SERT-Y) (*i.e.* a transporter construct predicted to produce strong homotypic FRET signals) (37).

Expression of C-SERT-Y and coexpression of C-DAT and Y-DAT resulted in enriched plasma membrane fluorescence (Fig. 4*A* and supplemental Fig. S1, respectively) and, as expected, robust N_{FRET} signals (0.712 ± 0.024 and 0.262 ± 0.017, respectively; Fig. 4*C*). Similarly, expression of fluorescently labeled GlyTs resulted in predominant plasma membrane fluorescence (Fig. 4*A* and supplemental Fig. S1). N_{FRET} values obtained with C-GlyT2 and Y-GlyT2 (0.268 ± 0.019; Fig. 4*C*) were similar to those found with C-DAT and Y-DAT. This confirms that GlyT2 forms oligomers in living cells. Although co-expression of C-GlyT1 and Y-GlyT1 produced a somewhat lower N_{FRET} value (0.206 ± 0.030; Fig. 4*C*), this value was significantly higher than that obtained with different membrane proteins employed as controls ($p < 0.001$; analysis of variance with Bonferroni correction). In accordance with the data shown in Fig. 3 and observations made with other members of the Na^+/Cl^--dependent neurotransmitter transporter family (9, 10), we also detected GlyT oligomers by FRET at intracellular locations (Fig. 4*A*; "cytosolic" N_{FRET} values: GlyT1, 0.196 ± 0.012; GlyT2, 0.283 ± 0.016). To validate our FRET data, we also employed a membrane-bound form of YFP that predominantly inserts into the plasma membrane (25); co-expression with C-GlyT2 yielded an N_{FRET} value of 0.152 ± 0.018 (Fig. 4*C* and supplemental Fig. S1). Apparently, this membrane-attached YFP can serve as an acceptor for CFP fluorophores attached to proteins integral to the plasma membrane; indeed, some spurious FRET signal was faintly visible upon co-expression with C-GlyT2 (Fig. 4*B* and supplemental Fig. S1). Therefore, we co-expressed both GlyT1 and GlyT2 with another unrelated membrane protein, the G-protein-coupled receptor for dopamine subtype 2, which had already served as a negative control in FRET studies on SERT and GAT1 (9). Similar to what was observed upon co-expression with the corticotropin-releasing factor receptor (CRFR1-Y; see Fig. 7*D*), co-expression of either C-GlyT1 or C-GlyT2 with dopamine subtype 2-Y resulted in significantly lower plasma membrane N_{FRET} values as compared with those obtained upon coexpressing CFP-

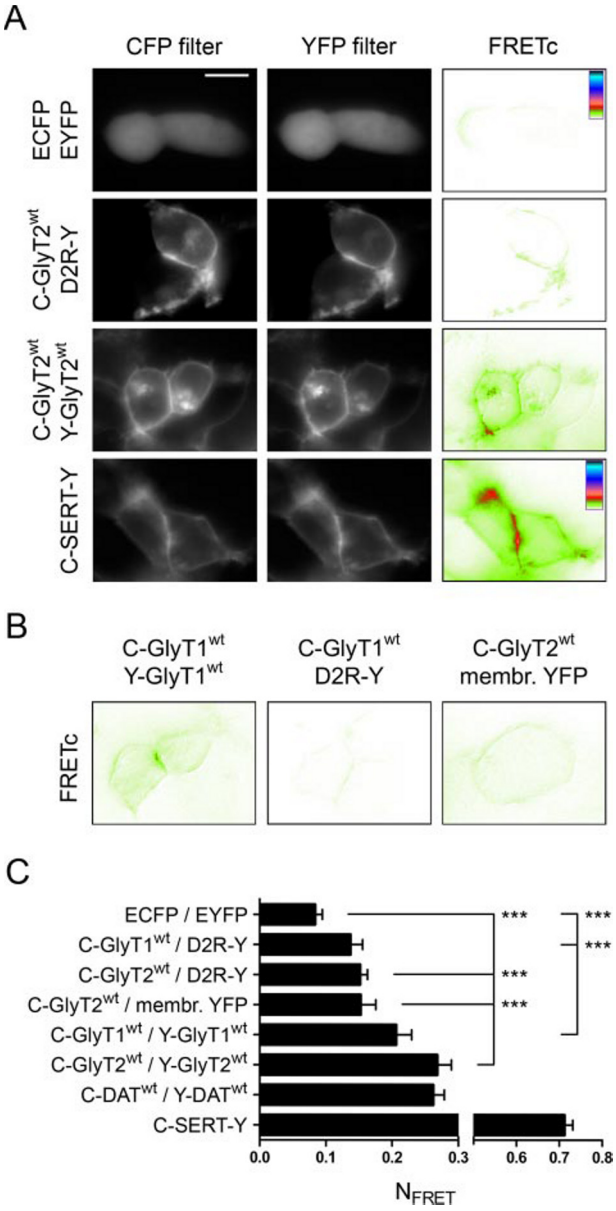

FIGURE 4. **GlyT oligomerization demonstrated by FRET in intact cells.** *A*, HEK 293T cells were transiently transfected with cDNAs encoding CFP- or YFP-tagged proteins as indicated. Two days after transfection, epifluorescence microscopy was performed; the *first* and *second columns* show *images* obtained with CFP and YFP filter sets, and the *third column* displays a corrected and inverted FRET image ($FRET_c$). A *look-up table* of the *color code* used is presented in the *first* and *fourth image*, *third column* (negative and positive control, respectively). All *images* shown are representative of 3–7 experiments. In all *images*, background fluorescence was subtracted. *Scale bar*, 10 μm. *B*, corrected and inverted FRET images of HEK 293T cells transiently transfected with the indicated constructs. For a *look-up table* of the *color code* used, see Fig. 5*A*. *Images* are representatives of at least three experiments. *C*, normalized FRET efficiencies (N_{FRET} values) are given for cells expressing the following constructs: enhanced cyan fluorescent protein (ECFP) and enhanced yellow fluorescent protein (EYFP) ($n = 124$), C-GlyT1 and D2R-Y ($n = 79$), C-GlyT2 and D2R-Y ($n = 50$), C-GlyT2b and membrane-bound YFP (*membr. YFP*; $n = 54$), C-GlyT1 and Y-GlyT1 ($n = 102$), and C-GlyT2 and Y-GlyT2 ($n = 73$), respectively. Similarly, HEK 293 cells expressing C-DAT and Y-DAT ($n = 30$) as well as C-SERT-Y ($n = 102$; see also Ref. 37) were examined. Data represent means ± S.E.; ***, $p < 0.001$; analysis of variance, *post hoc* Bonferroni's test for multiple comparisons.

and YFP-tagged GlyTs (0.137 ± 0.012 and 0.152 ± 0.015, respectively; $p < 0.001$; see Fig. 4, *A–C*, and supplemental Fig. S1). Together, these results confirm that both GlyTs oligomerize in intracellular compartments as well as at the plasma membrane.

Dimer Formation Revealed by Co-isolation of Differently Tagged GlyT2 Polypeptide—To prove that the putative $GlyT2^{T464C}$ dimer of 200 kDa contains two GlyT2 polypeptides, we used a co-isolation approach. To this end, we first singly transfected plasmids encoding His-$GlyT2^{T464C}$, Myc-$GlyT2^{WT}$, and Myc-$GlyT2^{T464C}$ into HEK 293T cells. Western blot analysis of detergent extracts prepared from the transfected cells with a GlyT2-specific antibody demonstrated that all of these tagged GlyT2 proteins were expressed at comparable levels (Fig. 5*A*, *lanes C1*, *L1*, and *L2*) and formed the previously described immunoreactive bands of 65 kDa corresponding to the core-glycosylated protein of 90 kDa, representing the mature monomer, and, in varying amounts, the 155-kDa dimer of the core-glycosylated GlyT2 (14). Upon coexpression of the His- and Myc-tagged transporters, no major changes in expression were detected (Fig. 5*A*, *lanes L3* and *L4*). After CuP treatment, GlyT2 adducts of 200 kDa were only seen in cells transfected with Myc- and/or His-$GlyT2^{T464C}$ mutant constructs (Fig. 5*A*, *lanes C2* and *L6–L8*), whereas samples from CuP-treated Myc-$GlyT2^{WT}$-expressing cells failed to produce this band (*lane L5*). Reprobing of the blots with a Myc-specific antibody revealed that both Myc-tagged transporters were expressed at similar levels when expressed individually (*lanes L9* and *L10*) or together with His-$GlyT2^{T464C}$ (*lanes L11* and *L12*). Upon CuP treatment, Myc immunoreactivity was incorporated into the 200 kDa band only in cells expressing the Myc-$GlyT2^{T464C}$ mutant (Fig. 5, *lanes L14* and *L16*) but not Myc-$GlyT2^{WT}$ (*lanes L13* and *L15*). Therefore, the GlyT2-immunoreactive 200 kDa band seen in *lane L7* represents a GlyT2 dimer consisting exclusively of His-$GlyT2^{T464C}$.

Subsequently, we used Ni^{2+}-NTA-agarose beads to isolate His-GlyT2 and associated proteins from the detergent extracts of the single- and double-transfected cells. The agarose-bound proteins were then eluted and subjected to Western blot analysis. Fig. 5*B* shows that GlyT2 protein was efficiently affinity-isolated from detergent extracts prepared from His-GlyT2-expressing cells (*lanes E3*, *E4*, *E7*, and *E8*). No GlyT2 immunoreactivity was found in samples isolated from cells transfected only with Myc-tagged GlyT2 constructs (*lanes E1*, *E2*, *E5*, and *E6*), consistent with a specific binding of the His tag to the Ni^{2+}-NTA-agarose. Reprobing of the blot membranes with a Myc-specific antibody revealed that affinity purification on Ni^{2+}-NTA-agarose co-isolated core-glycosylated monomeric and dimeric Myc-tagged GlyT2 protein (65 and 155 kDa) from cells expressing both His-$GlyT2^{T464C}$ and Myc-$GlyT2^{WT}$ or Myc-$GlyT2^{T464C}$ and that this co-isolation was independent of CuP treatment (Fig. 5*B*, *lanes E11*, *E12*, *E15*, and *E16*). This result confirms that core-glycosylated GlyT2 forms stable oligomers intracellularly (see also Ref. 14 and Fig. 3), thus allowing the co-isolation of Myc-GlyT2 protein. Furthermore, incorporation of Myc immunoreactivity into the 155-kDa band suggests that this band is indeed a GlyT2 dimer, which contains both His-$GlyT2^{T464C}$ and Myc-GlyT2 protein.

Upon cotransfection of the His-$GlyT2^{T464C}$ mutant with Myc-$GlyT2^{WT}$ followed by CuP treatment, Myc immunoreactivity was not found at 200 kDa (Fig. 5*B*, *lane E15*), although

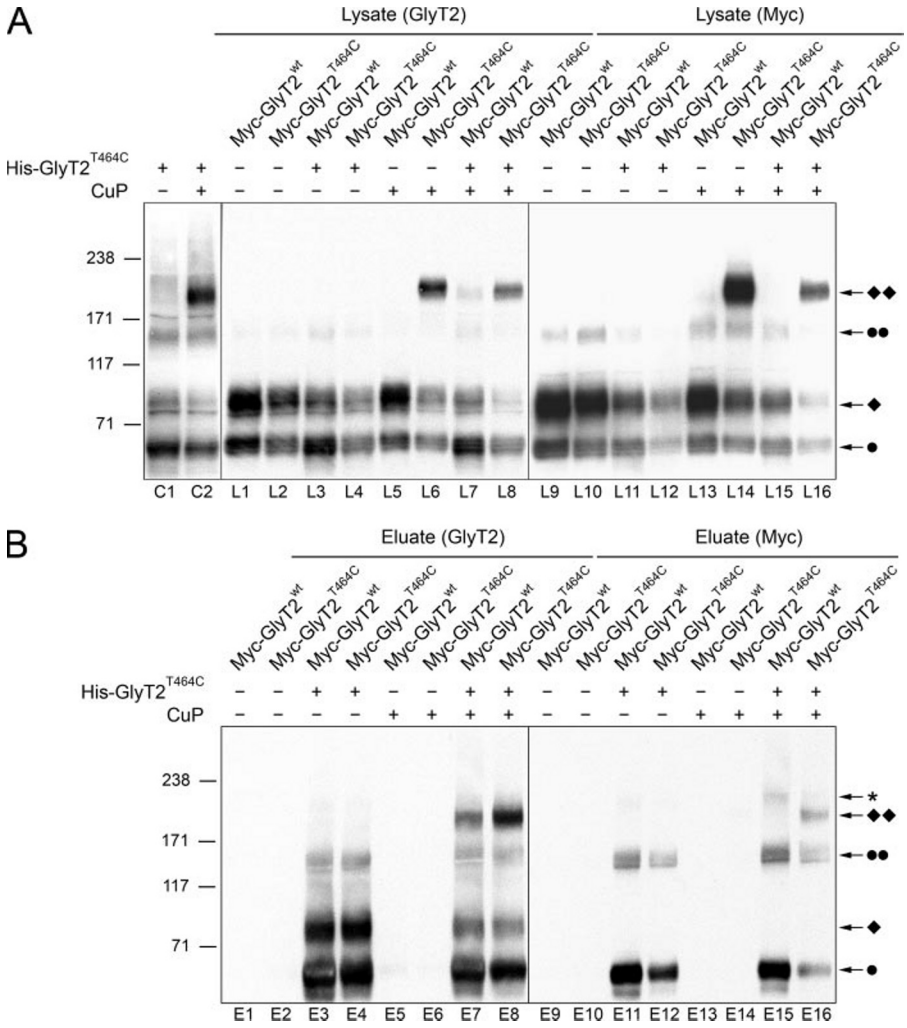

FIGURE 5. **The 200-kDa CuP-induced GlyT2 adduct is a homodimer.** HEK 293T cells cotransfected with His-GlyT2^{T464C} and either Myc-GlyT2^{WT} or Myc-GlyT2^{T464C} were treated with CuP (+) or PBS (−) as indicated. *A*, aliquots of detergent extracts prepared from the treated cells were sequentially analyzed by Western blotting using the GlyT2-specific antibody (*lanes C1*, *C2*, and *L1–L8*) and, after removal of bound antibody, an anti-Myc antibody (*lanes L9–L16*). Note the presence of mature GlyT2 dimers in *lanes L6–L8* and *L14* and *L16*, respectively. *B*, aliquots of the extracts used in *A* were affinity-purified on Ni^{2+}-NTA-agarose. Blots prepared from the eluates were first probed with the GlyT2 antibody (*lanes E1–E8*) and, after removal of the bound antibodies, restained with a Myc-specific antibody (*lanes E9–E16*). Note that a Myc-immunoreactive 200-kDa adduct was isolated only after CuP treatment of cells expressing both His-GlyT2^{T464C} and Myc-GlyT2^{T464C} (*lane E16*). The different transporter forms are indicated: ●, immature monomer; ◆, mature monomer; ●●, immature dimer; ◆◆, mature dimer. An *asterisk* indicates an unspecific band detected with the anti-Myc antibody.

some reactive 200-kDa complex had been isolated (compare *lanes L7* and *E7*). An additional Myc-immunoreactive band at 220 kDa (*lane E15*, *) did not react with the GlyT2 antibody and thus represents an unknown cross-reactive protein complex presumably derived from endogenous HEK 293T cell proteins. Incorporation of Myc immunoreactivity into the cross-linked 200-kDa GlyT2 complex was only observed when His-GlyT2^{T464C} and Myc-GlyT2^{T464C} were coexpressed (Fig. 5, *lane E16*). These data prove that the band at 200 kDa represents a GlyT2 dimer, which is covalently stabilized by the CuP-induced disulfide bond. Since dimer formation of complex-glycosylated GlyT2 proteins required the presence of the T464C substitution in both tagged proteins, disulfide bonding apparently involves Cys^{464} exclusively, consistent with transporter dimerization involving identical interfaces.

GlyT2 Can Form Hetero-oligomers with Other Members of the SLC6a Family—Given the high degree of overall homology between the different transporter subtypes in the SLC6a family, we surmised that they might also form hetero-oligomeric complexes. Hence, we searched for resonance energy transfer between GlyT2 and DAT or GAT1. Co-expression of C-DAT with Y-GlyT2 resulted in a FRET signal at the plasma membrane level (Fig. 6*A*; $N_{FRET} = 0.25 \pm 0.02$), which was comparable with that detected with homotypic GlyT2- or DAT-expressing cells ($N_{FRET} = 0.31 \pm 0.03$ and 0.26 ± 0.02, respectively; Fig. 6*B*). Similar results were obtained with cells expressing C-GAT1 and Y-GlyT2 ($N_{FRET} = 0.28 \pm 0.01$; Fig. 6, *A* and *B*), confirming that GlyT2 forms hetero-oligomers with other members of the SLC6a family.

To further investigate whether this oligomerization is mediated via an interface close to threonine 464 in GlyT2, we performed co-isolation experiments with cells expressing both GlyT2^{T464C} and/or His-DAT^{WT} with and without CuP-induced cross-linking. As expected, Western blot analysis of detergent extracts from these cells revealed GlyT2 immunoreactivity only in cells transfected with the GlyT2^{T464C} expression construct (Fig. 6*C*, *lanes L2*, *L3*, *L5*, and *L6*), although coexpression with His-DAT^{WT} resulted in a reduction of GlyT2^{T464C} expression. Similarly, DAT immunoreactivity was only detected in lanes loaded with detergent extracts from His-DAT^{WT}-transfected cells (Fig. 6*C*, *lanes L7*, *L8*, *L10*, and *L11*). Dimers of the expected sizes were detected after treatment of the cells with CuP (Fig. 6*C*, *lanes L5*, *L6*, *L10*, and *L11*). However, coexpression of His-DAT^{WT} and GlyT2^{T464C} failed to produce additional GlyT2- and DAT-immunoreactive bands, demonstrating that the predominant dimers formed were homodimers consisting of His-DAT^{WT} or GlyT2^{T464C}. These detergent extracts were subsequently subjected to Ni^{2+}-NTA-agarose affinity purification of His-tagged proteins. Western blots of the respective eluates showed that DAT immunoreactivity was efficiently enriched in samples from His-DAT^{WT}-expressing cells (Fig. 6*C*, *lanes E7*, *E8*, *E10*, and *E11*). GlyT2 immunoreactivity was only detected in eluates from cells co-expressing His-DAT^{WT} and GlyT2^{T464C} (Fig. 6*C*, *lanes E2* and

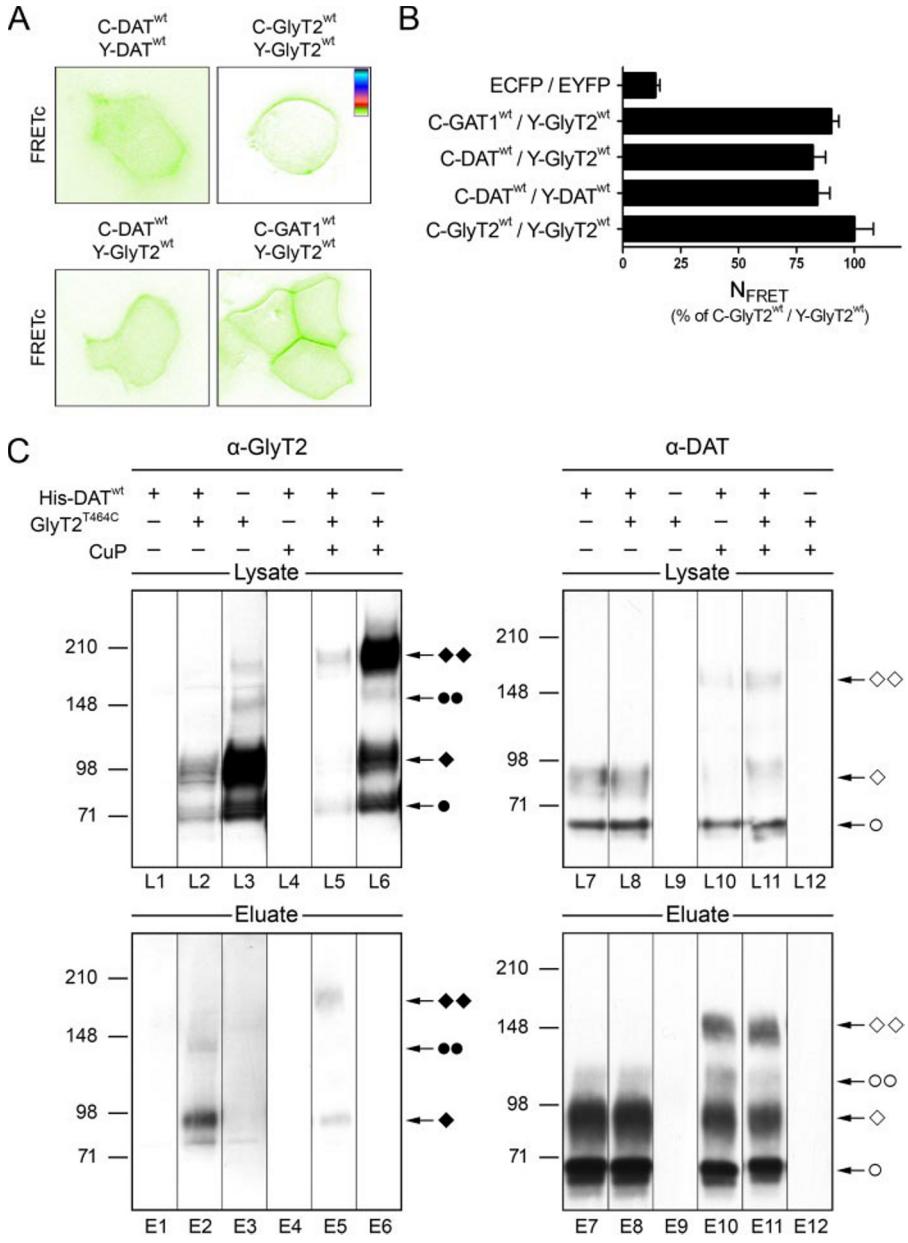

FIGURE 6. **Heteromer formation of GlyT2 with DAT and GAT1.** *A*, HEK 293T cells were transiently transfected with cDNAs encoding CFP- or YFP-tagged proteins, as indicated. Two days after transfection, $FRET_c$ values were obtained. A look-up table of the color code used is given in the upper right. N_{FRET} values (percentage) normalized to C-GlyT2/Y-GlyT2-expressing cells (100%) are given for cells expressing ECFP and EYFP ($n = 16$), C-GAT^{WT} and Y-GlyT2 ($n = 34$), C-DAT^{WT} and Y-$GlyT2^{WT}$ ($n = 34$), C-DAT^{WT} and Y-DAT^{WT} ($n = 30$), and C-$GlyT2^{WT}$ and Y-$GlyT2^{WT}$ ($n = 18$), respectively. Note that N_{FRET} values obtained from C-$GlyT2^{WT}$/Y-$GlyT2^{WT}$-expressing cells were not significantly different statistically from that of cells expressing C-GAT^{WT}/Y$GlyT2^{WT}$ or C-DAT^{WT}/Y-$GlyT2^{WT}$ ($p > 0.05$). Data represent means ± S.E. analysis of variance with post hoc Bonferroni's test for multiple comparison. *C*, HEK 293T cells were transfected with His-DAT^{WT}, $GlyT2^{T464C}$, or both constructs and treated with CuP (+) or PBS (−), and detergent extracts prepared from these cells were analyzed by Western blotting with the GlyT2 antibody (*lanes L1–L6*), followed, after removal of the bound antibodies, by an anti-DAT antibody (*lanes L7–L12*). Aliquots of the detergent extracts were subjected to Ni^{2+}-NTA-based purification of His-tagged proteins. The eluates from the beads were sequentially analyzed by Western blotting using first the anti-GlyT2 (*lanes E1–E6*) and then the anti-DAT antibody (*lanes E7–E12*). Note that in the eluates, GlyT2 immunoreactivity was only found in fractions derived from His-DAT^{WT}- and $GlyT2^{T464C}$-co-expressing cells and that both the mature monomer and the cross-linked dimer were present in these fractions. Different transporter forms are indicated. ●, immature monomer; ♦, mature monomer; ●●, immature dimer; ♦♦, mature dimer. *Filled symbols*, GlyT2; *open symbols*, DAT.

E5), whereas the other lanes were devoid of specific signals, indicating that co-isolation was dependent on His-DAT^{WT}. Thus, these results confirm the data obtained by FRET microscopy. Surprisingly, both *lanes* showed a band of ~90 kDa, resembling the mature $GlyT2^{T464C}$ monomer, whereas immature forms of the transporter (*i.e.* the intracellular immature monomer and its dimer) were excluded from this fraction. In addition to this band, eluates prepared from $GlyT2^{T464C}$/His-DAT^{WT}-expressing cells produced another GlyT2-immunoreactive band at ~200 kDa after treatment with CuP. Its position corresponds to that of the mature GlyT2 dimer (Fig. 6*C*, *lane E5*) and is clearly distinct from the DAT-immunoreactive bands in the same sample (Fig. 6*C*, *lane E11*). Taken together, these data reveal that the mature $GlyT2^{T464C}$ protein can form a dimer or higher order oligomer with His-DAT^{WT}. However, these heteromeric $GlyT2^{T464C}$-DAT^{WT} complexes form only with low efficacy and cannot be cross-linked by CuP, suggesting that their structure differs from that of the respective homodimers.

A Mutation Impairing Dimerization Results in Intracellular Retention of GlyT2—In order to identify residues other than Thr^{464} that might contribute to the putative dimer interface of GlyT2, we examined our structural model for neighboring residues. A candidate residue likely to contribute to the dimerization interface was found to be residue Trp^{469}, located after the end of EL3 at the beginning of TM6. In the model shown in Fig. 1, this residue is predicted to contact the neighboring transporter monomer. We therefore generated a double mutant C-$GlyT2^{T464C/W469R}$, in which the hydrophobic tryptophan residue had been replaced by a charged arginine side chain. This substitution caused intracellular retention of mutant GlyT2, as observed by confocal microscopy employing trypan blue to specifically stain the plasma membrane of living cells (Fig. 7*A*). In contrast, GlyT2s containing the single substitution T464C or T457K were expressed at the cell surface to an extent indistinguishable from that seen with $GlyT2^{WT}$ (not shown, but see Fig. 7*B*). Both C-$GlyT2^{T464C}$ and C-$GlyT2^{T457K}$ colocalized with Y-$GlyT2^{WT}$ at the plasma membrane upon co-expression,

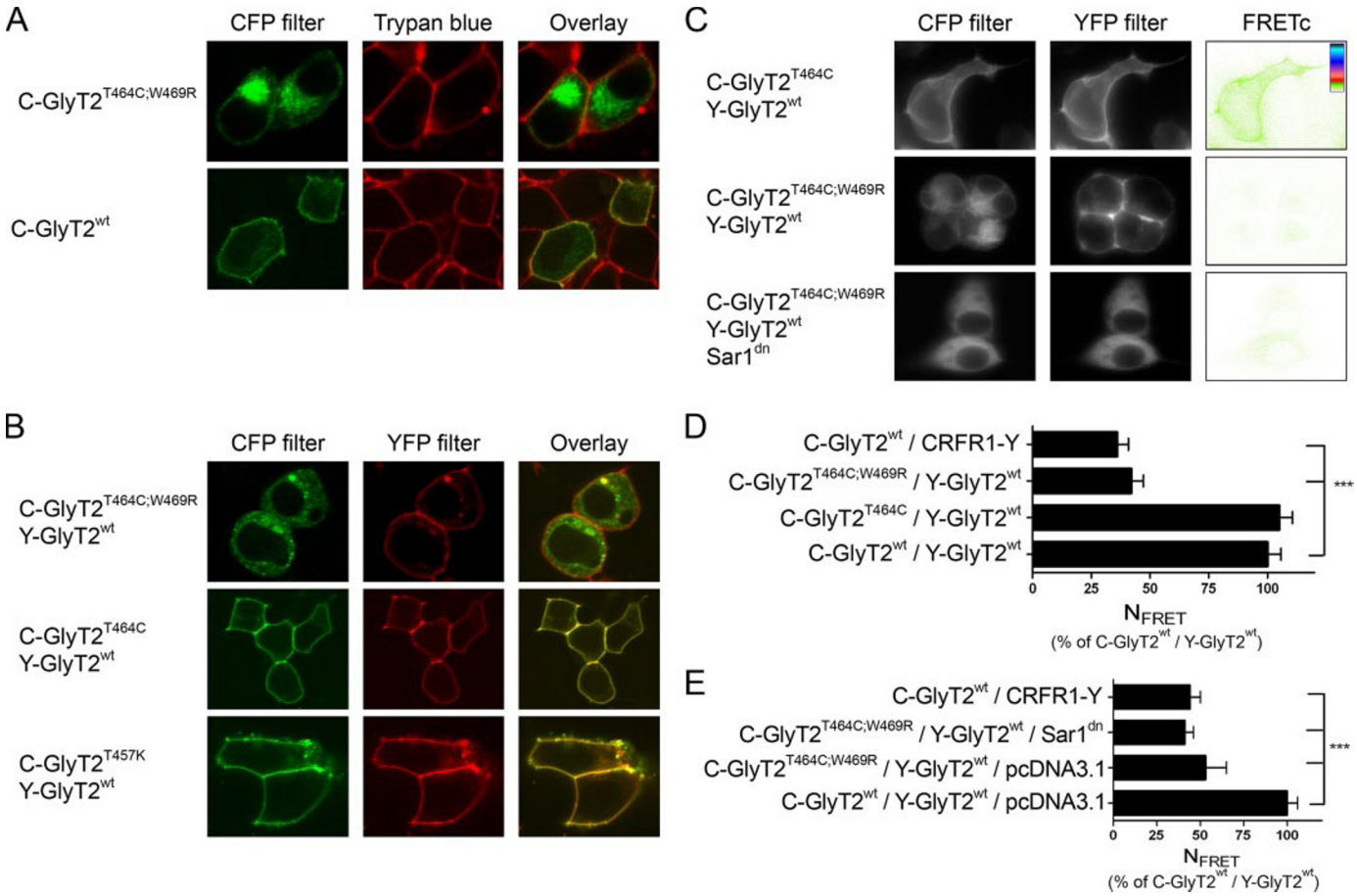

FIGURE 7. **Disruption of GlyT2 dimerization leads to intracellular retention.** HEK 293T cells were transiently transfected with C-GlyT2^{WT} and C-GlyT2 mutants as indicated and examined using a confocal microscope (*A* and *B*) or an epifluorescence microscope (*C*). *A*, colocalization of C-GlyT2$^{T464C/W469R}$ and C-GlyT2^{WT} with trypan blue; fluorescence emitted by CFP and trypan blue is shown in *green* and *red*, respectively. *B*, colocalization of C-GlyT2 mutants and Y-GlyT2^{WT}, as indicated. The *pictures* shown in *A* and *B* are representative of four or five images captured in parallel from the same transfection; the experiments were repeated two or three times with independent transfections. *C*, representative images obtained with CFP and YFP filter sets; the *third column* displays FRET$_c$ for HEK 293T cells expressing C-GlyT2$^{T464C/W469R}$ and Y-GlyT2^{WT} (*upper lane*) or C-GlyT2$^{T464C/W469R}$ and Y-GlyT2^{WT} without and with dominant negative Sar1^{dn} (*lower lanes*). *D*, N_{FRET} values, normalized to C-GlyT2^{WT}/Y-GlyT2^{WT}-expressing cells, are indicated for cells co-expressing C-GlyT2^{WT} and CRFR1-Y (n = 30), C-GlyT2$^{T464C/W469R}$ and YFP-GlyT2^{WT} (n = 54), C-GlyT2^{T464C} and Y-GlyT2^{WT} (n = 67), and C-GlyT2^{WT} and Y-GlyT2^{WT} (n = 62), respectively. Data represent means ± S.E. of three experimental days. *E*, N_{FRET} values (percentage) normalized to C-GlyT2^{WT}/Y-GlyT2^{WT} expressing cells are indicated for cells co-expressing C-GlyT2^{WT} and CRFR1-Y and pcDNA3.1 (n = 14), C-GlyT2$^{T464C/W469R}$ and Y-GlyT2^{WT} and Sar1^{dn} (n = 17), C-GlyT2$^{T464C/W469R}$ and Y-GlyT2^{WT} and pcDNA3.1 (n = 16), and C-GlyT2^{WT} and Y-GlyT2^{WT} and pcDNA3.1 (n = 25). Data represent means ± S.E. of two experimental days. ***, $p < 0.001$; analysis of variance, *post hoc* Bonferroni's test for multiple comparisons.

whereas C-GlyT2$^{T464C/W469R}$ colocalized only weakly in intracellular compartments (Fig. 7*B*). Importantly, this double mutant was incapable of retaining Y-GlyT2^{WT} intracellularly. In analogy to retention assays employed with SERT (37) and DAT (38), this served as the first indication that this double mutant dimerizes only poorly. Subsequently, we co-expressed C-GlyT2$^{T464C/W469R}$ with Y-GlyT2^{WT} and performed FRET microscopy. Fig. 7, *C* and *D*, shows clearly that the FRET signal in intracellular compartments was greatly reduced (N_{FRET} = 42 ± 5% of N_{FRET} *C-GlyT2WT/Y-GlyT2WT*) as compared with that observed in C-GlyT2^{WT} and Y-GlyT2^{WT} (not shown, but see Fig. 4) but similar to that found in C-GlyT2^{WT}- and CRFR1-Y co-expressing cells (Fig. 7, *D* and *E*). In contrast, FRET microscopy performed with C-GlyT2^{T464C} co-expressed with Y-GlyT2^{WT} or transfections of CFP- and YFP-tagged versions of GlyT2^{T457K} revealed FRET signals comparable with those seen with CFP- and YFP-tagged GlyT2^{WT} (N_{FRET} = 105 ± 5% and N_{FRET} = 94 ± 4% (Fig. 7, *C* and *D*); see also Fig. S1). We also induced intracellular retention of Y-GlyT2^{WT} by co-expressing Sar1^{dn}, a T39N mutant of Sar1a that impairs the correct formation of vesicles mediating endoplasmic reticulum export of protein cargo (39), in order to exclude the possibility that low FRET signals resulted from a lack of colocalization. HEK 293 cells triple-transfected with Y-GlyT2^{WT}, C-GlyT2$^{T464C/W469R}$, and Sar1^{dn} showed intracellular retention of both the wild-type transporter and the double mutant (Fig. 7*C*). Although massive intracellular accumulation of the two proteins was observed, we failed to detect a specific intracellular FRET signal in these cells (N_{FRET} = 41 ± 5% as compared with N_{FRET} of C-GlyT2^{WT}- and Y-GlyT2^{WT}-expressing cells; Fig. 7*E*). This result further indicates that the GlyT2$^{T464C/W469R}$ mutant is unable to oligomerize and is retained intracellularly.

To biochemically prove that GlyT2$^{T464C/W469R}$ is indeed unable to dimerize, a Myc-tagged version of the mutant protein was co- expressed with His-GlyT2^{T464C}. Western blot analysis of detergent extracts prepared from cells expressing His-GlyT2^{T464C}, Myc-GlyT2$^{T464C/W469R}$, or both constructs

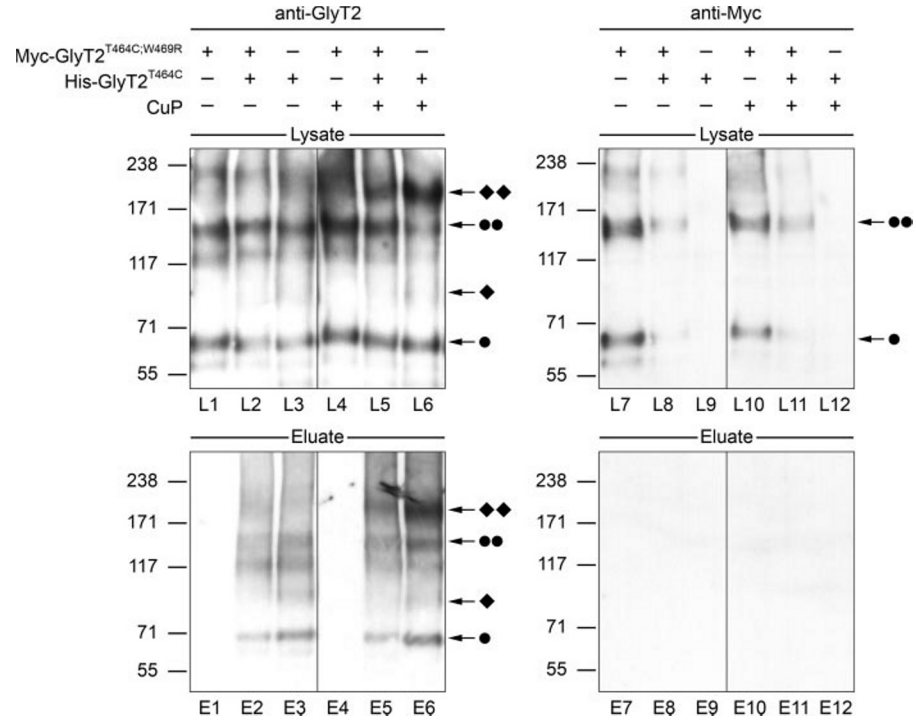

FIGURE 8. **GlyT2$^{T464C/W469R}$ does not form complexes with GlyT2^{T464C}.** *A*, HEK 293T cells were transfected with His-GlyT2^{T464C}, Myc-GlyT2$^{T464C/W469R}$, or both constructs. After 48 h, the cells were treated with CuP (+) or PBS (−). Detergent extracts prepared from these cells were sequentially analyzed by Western blotting with first the anti-GlyT2 antibody and then anti-Myc antibody. *B*, aliquots of the detergent extracts were subjected to Ni^{2+}-NTA affinity purification of His-tagged proteins. Western blots of the eluates were analyzed by using first anti-GlyT2 and then anti-Myc antibodies. Note that no Myc immunoreactivity was found in the eluates prepared from cells co-expressing His-GlyT2^{T464C} and Myc-GlyT2$^{T464C/W469R}$, although purification of His-GlyT2^{T464C} was successful, as indicated by GlyT2 immunoreactivity (*lower panel*, *left*). The different transporter forms are indicated as follows. ●, immature monomer; ◆, mature monomer; ●●, immature dimer; ◆◆, mature dimer.

revealed strong GlyT2 immunoreactivity in all three samples (Fig. 8*A*, *lanes L1–L3*). Upon CuP treatment, a strong GlyT2-immunoreactive band at 200 kDa was seen in His-GlyT2^{T464C}-expressing (*lanes L5* and *L6*) but not Myc-GlyT2$^{T464C/W469R}$-expressing cells (*lane L4*). Reprobing of these blots with a Myc-specific antibody revealed immunoreactive bands in all lanes loaded with extracts prepared from Myc-GlyT2$^{T464C/W469R}$-expressing cells (Fig. 8, *lanes L7*, *L8*, *L10*, and *L11*). Consistent with our findings using confocal microscopy, we failed to detect any mature forms of the transporter; only the intracellular monomer or its dimer could be detected in these *lanes*. Aliquots of these extracts were then subjected to Ni^{2+}-NTA affinity purification of His-GlyT2^{T464C}. Probing Western blots prepared from these eluates with the GlyT2 antibody revealed immunoreactive bands for the intracellular monomer and its dimer, the mature monomer, and, in samples prepared from CuP-treated cells, also the mature dimer, in the His-GlyT2^{T464C}-containing samples (Fig. 8*B*, *lanes E2*, *E3*, *E5*, and *E6*). Reprobing of these Western blots with Myc-specific antibodies consistently failed to produce any specific band (Fig. 8*B*, *lanes E7–E12*), indicating that even in intracellular compartments, Myc-GlyT2$^{T464C/W469R}$ does not interact with His-GlyT2^{T464C}. We therefore conclude that EL3 and the beginning of TM6 (*i.e.* the region containing the crucial residues Thr^{464} and Trp^{469}) is important for GlyT2 dimerization.

DISCUSSION

In this study, we used two independent approaches, cysteine-mediated cross-linking and FRET microscopy, to show that upon heterologous expression both GlyT2 and GlyT1 form dimers in the plasma membrane. Comparison with other members of the SLC6a family suggests that GlyTs oligomerize via an interface that is conserved between SLC6a members.

Based on oxidative cross-linking data obtained with the DAT and GlyT models generated by using the crystal structure of the bacterial homolog $LeuT_{Aa}$ as a template, we focused on EL3 linking TM5 and TM6 as contributing to a potential oligomerization interface. This loop is located at the outer surface of the transporter monomer above TM11 and, in the DAT, contains residue Cys^{306}, which is responsible for oxidative cross-linking of the transporter dimer (6). Here, modeling predicted the GlyT positions homologous to Cys^{306} of the DAT, Thr^{464} in GlyT2, and Leu^{343} in GlyT1c to similarly face a conserved dimerization interface of the transporters that might involve residues within EL3, the beginning of TM6, and possibly TM11. Indeed, upon cysteine substitution and oxidizing treatment, GlyT2^{T464C} and GlyT1^{L343C} were efficiently cross-linked to 200- and 190-kDa adducts, respectively. In contrast, neither GlyT1^{WT} nor GlyT2^{WT} nor other cysteine-substituted GlyT2 proteins (GlyT2^{K462C} and GlyT2^{T557C}) produced the 200 kDa band upon CuP treatment. Furthermore, in the case of GlyT1, a double mutant (GlyT1$^{C116A/L343C}$), in which a second extracellular cysteine at position 116 had been replaced by alanine, was found to be as efficiently cross-linked as GlyT1^{L343C}. All of these data are consistent with a high positional specificity of cysteine-mediated cross-linking at an interface formed by EL3. Cross-linking did not significantly affect transporter function, as demonstrated by recordings from GlyT2^{T464C}-expressing oocytes prior to and after CuP treatment. This is consistent with the idea that the dimerization interface does not undergo major structural rearrangements during the transport cycle. Also, reduction of the cross-linked transporter dimer with β-mercaptoethanol resulted in a cleavage of the 200-kDa adduct, indicating that CuP treatment did not induce aggregation of the GlyT2^{T464C} mutant.

The differential sensitivity to endoglycosidase H and peptide: *N*-glycosidase F treatment as well as our surface biotinylation experiments indicated that the CuP-cross-linked cysteine-substituted GlyT2 adducts of 200 kDa correspond to dimers com-

posed of complex-glycosylated, mature transporter polypeptides located in the plasma membrane. Since detection of these 200 kDa GlyT2 dimers by SDS-PAGE was stringently dependent on CuP cross-linking, its constituent monomers appeared to be only loosely associated. This is consistent with blue native PAGE experiments in which we failed to detect electrophoresis-resistant GlyT oligomers at the cell surface of both oocytes and HEK 293 cells (see Ref. 14).[6] Also, in sedimentation studies, detergent-solubilized GlyT1 behaves as a monomeric protein (40). In line with our previous data (14), we found dimers of immature core-glycosylated transporters that were localized intracellularly, as revealed by their inaccessibility to surface biotinylation. Notably, these intracellular GlyT complexes displayed partial resistance toward dissociation by SDS, and CuP treatment did not increase their abundance. This may in part be due to inefficient permeation of CuP into the cytosol. Alternatively, a different orientation of the EL3 cysteine in the immature GlyT2^{T464C} polypeptide might impede cross-linking. The differences noted in the SDS resistance of mature *versus* immature GlyT2 complexes might even reflect distinct steps in intracellular transporter processing. The complex carbohydrate side chains that are added and modified posttranslationally might weaken the interactions between dimerization interfaces and thereby result in a detergent-sensitive dimer upon plasma membrane incorporation. Indeed, evidence for a role of glycosylation in transporter processing and stability has been obtained in studies showing reduced transport activity upon mutation of the transporters' *N*-glycosylation sites (41, 42).

Direct support for the existence of GlyT oligomers in living cells comes from our FRET data. Consistent with our biochemical results, a specific FRET signal was seen upon co-expression of CFP- and YFP-tagged GlyT1 or GlyT2 polypeptides in both the plasma membrane and intracellular compartments. During revision of this manuscript, a very similar result with GlyT1 has been reported by others (43). Differences found in FRET signal intensities between the two transporters (see Fig. 4) may reflect differences in expression levels and/or membrane targeting as well as different orientations of the fluorophores, due to the different sizes of the N-terminal domains to which the fluorophores were attached.

That the CuP-induced GlyT complexes are indeed homodimers was proven here by co-isolation of the differentially tagged transporter polypeptides. This and its size of about 200 kDa indicate that the cross-linked GlyT2 dimer contains no other additional polypeptides. Since our co-isolation protocol produced dimers only when both monomers carried the T464C substitution, we conclude that this particular cysteine is required and sufficient for complex stabilization by intermolecular disulfide bonding. Our results indicate that the transporter monomers dimerize via an interface that is conserved between the GlyTs and the DAT (5, 6) and possibly also other SLC6a family members. For the DAT, it has been reported that a second cysteine, located within TM4, also allows intermolecular cross-linking. This cysteine is conserved between DAT and the GlyTs (Cys^{393} in GlyT2 and Cys^{220} in GlyT1, respectively). However, under our experimental conditions, we consistently failed to detect the formation of any higher molecular weight adducts with the respective wild-type constructs. This indicates that within the GlyTs, this cysteine is not accessible for intermolecular cross-linking.

In addition to the homodimers described above, heteromer formation between GlyT2 and GAT1, or DAT, was seen by both FRET analysis and co-purification of GlyT2^{T464C} immunoreactivity with His-DAT^{WT} on Ni^{2+}-NTA-agarose. However, this co-isolation was completely independent of CuP cross-linking, since we failed to detect any cross-linked heterodimers in eluates from Ni^{2+}-NTA columns. Furthermore, we only found the fully glycosylated GlyT2 polypeptide in these eluates, whereas immature transporter forms were excluded from this fraction; this suggests that heterodimerization occurs at the plasma membrane. Together with the observation that even the cross-linked GlyT2^{T464C} dimer was co-isolated with His-DAT^{WT}, we conclude that CuP-induced intermolecular cross-linking is selective for each SLC6a transporter subtype. This conclusion implies that the interaction of His-DAT^{WT} with the complex glycosylated GlyT2 monomer and dimer involves interaction sites distinct from that mediating dimer formation. It is tempting to speculate that such interaction sites could allow the formation of higher order transporter oligomers at sites of high transporter density, such as the presynaptic terminal membrane.

Based on our modeling data, we propose that the SLC6a transporters dimerize via an interface to which the EL3 region and the extracellular end of TM6 contribute. Support for this proposal comes from our analysis of the GlyT2$^{T464C/W469R}$ double mutant, which carries a positive charge instead of a tryptophan at the extracellular end of TM6 (see Fig. 1, *D* and *E*). This mutant transporter protein was found to be deficient in dimerization as shown by (i) the low of FRET signal resulting upon co-expression with GlyT2^{WT}, (ii) impaired co-isolation with the GlyT2^{T464C} mutant, and (iii) the inability to retain GlyT2^{WT} intracellularly. We also tried to identify determinants for dimerization within TM11, which according to our model is closest to the dimerization interface. However, substitutions of aromatic residues within TM11 by branched aliphatic amino acids failed to reduce CuP cross-linking of the respective mutants,[7] indicating that these side chains are not specific determinants of transporter oligomerization. Taken together, our data suggest that GlyTs dimerize via an interface involving EL3 and the extracellular end of TM6. Disruption of this interface results in dimerization- deficient transporter protein that is retained intracellularly.

In addition to the dimerization interface defined by EL3 and the extracellular end of TM6, other putative oligomerization domains have been described in earlier studies of other SLC6a family members. First, a leucine heptad motif within TM2 of GAT1 has been found to be essential for both plasma membrane insertion and oligomerization of the transporter (11). According to our structural models, these leucines as well as glutamate and tyrosine residues that also have been proposed to

[6] I. Bartholomäus and A. Nicke, unpublished data.

[7] V. Eulenburg, unpublished data.

be important for oligomerization (12) are at least partially buried within the transporter structure and thus unlikely to directly participate in oligomer formation (see also Ref. 4). Presumably, substitutions at these positions lead to structural changes that indirectly disturb the dimerization interface. Similarly, the glycophorin A homology motif, which has been identified in TM6 of the DAT in close proximity to EL3 (38), is predicted to lie within the central core of the transporter close to the substrate binding site and thus is unlikely to directly contribute to monomer interactions. Presumably, these mutations affect folding or proper tertiary structure acquisition and thus cause a loss of function and/or intracellular retention of the transporters. Also, it is noteworthy that $LeuT_{Aa}$ has been crystallized in dimeric structural form. In this bacterial homolog, a homomeric dimerization interface is formed by TM9 and TM12 (*i.e.* a region that, based on retention assays with partial transporter constructs, has also been suggested to serve as a dimerization domain in the human SERT) (37).

Oligomerization of SLC6a transporter proteins has been proposed to be important for both posttranslational processing and transporter function at the plasma membrane (4, 8). In different studies, truncated or mutated transporter fragments, which are retained intracellularly, have been shown to exert dominant negative effects on co-expressed full-length transporters. For example, the expression of SERT fragments containing TM1 and -2, TM5 and -6, or TM11 and -12 resulted in intracellular retention of the co-expressed full-length SERT (37). In the case of the NET, a heterozygous mutation (A457P), which is causal for orthostatic intolerance in human patients, has been found to cause a 90% reduction of NET activity (44). Similar effects have also been described for GlyT2. There, a disease mutation that is associated with human hyperekplexia (S510R), resulted in intracellular retention of the co-expressed wild-type transporter (45). Taken together, the existence of such dominant mutations corroborates the conclusions reached in this study. Similar to other members of the SLC6a family, GlyTs form dimers, and dimer formation appears to be a prerequisite for correct transporter processing and surface delivery. At the cell surface, transporter oligomerization may have functional consequences (8). For monoamine transporters, oligomerization has been suggested to support their reverse operation (30). Although the stabilization of the $GlyT2^{T464C}$ dimer by CuP-induced cross-linking did not affect transport activity, we cannot exclude modulatory effects of dimerization on transport activity, since the dimerization-deficient $GlyT2^{T464C/W469R}$ mutant was retained intracellularly and hence not accessible to functional characterization. Clearly, further experiments are required to unravel the precise mechanisms by which oligomerization affects transporter surface expression and/or activity.

Acknowledgments—We thank Drs. Marc G. Caron, Wencke Armsen, and Viacheslav Nikolaev for kindly providing expression plasmids for DAT, GlyT2, and membrane-bound YFP, respectively, and M. Krause for excellent technical assistance.

REFERENCES

1. Torres, G. E., Gainetdinov, R. R., and Caron, M. G. (2003) *Nat. Rev. Neurosci.* **4,** 13–25
2. Gether, U., Andersen, P. H., Larsson, O. M., and Schousboe, A. (2006) *Trends Pharmacol. Sci.* **27,** 375–383
3. Eulenburg, V., Armsen, W., Betz, H., and Gomeza, J. (2005) *Trends Biochem. Sci.* **30,** 325–333
4. Farhan, H., Freissmuth, M., and Sitte, H. H. (2006) *Handb. Exp. Pharmacol.* 233–249
5. Hastrup, H., Karlin, A., and Javitch, J. A. (2001) *Proc. Natl. Acad. Sci. U. S. A.* **98,** 10055–10060
6. Hastrup, H., Sen, N., and Javitch, J. A. (2003) *J. Biol. Chem.* **278,** 45045–45048
7. Jess, U., Betz, H., and Schloss, P. (1996) *FEBS Lett.* **394,** 44–46
8. Kilic, F., and Rudnick, G. (2000) *Proc. Natl. Acad. Sci. U. S. A.* **97,** 3106–3111
9. Schmid, J. A., Scholze, P., Kudlacek, O., Freissmuth, M., Singer, E. A., and Sitte, H. H. (2001) *J. Biol. Chem.* **276,** 3805–3810
10. Sorkina, T., Doolen, S., Galperin, E., Zahniser, N. R., and Sorkin, A. (2003) *J. Biol. Chem.* **278,** 28274–28283
11. Scholze, P., Freissmuth, M., and Sitte, H. H. (2002) *J. Biol. Chem.* **277,** 43682–43690
12. Korkhov, V. M., Farhan, H., Freissmuth, M., and Sitte, H. H. (2004) *J. Biol. Chem.* **279,** 55728–55736
13. Yamashita, A., Singh, S. K., Kawate, T., Jin, Y., and Gouaux, E. (2005) *Nature* **437,** 215–223
14. Horiuchi, M., Nicke, A., Gomeza, J., Aschrafi, A., Schmalzing, G., and Betz, H. (2001) *Proc. Natl. Acad. Sci. U. S. A.* **98,** 1448–1453
15. Lopez-Corcuera, B., Alcantara, R., Vazquez, J., and Aragon, C. (1993) *J. Biol. Chem.* **268,** 2239–2243
16. Haugeto, O., Ullensvang, K., Levy, L. M., Chaudhry, F. A., Honore, T., Nielsen, M., Lehre, K. P., and Danbolt, N. C. (1996) *J. Biol. Chem.* **271,** 27715–27722
17. Gomeza, J., Hulsmann, S., Ohno, K., Eulenburg, V., Szoke, K., Richter, D., and Betz, H. (2003) *Neuron* **40,** 785–796
18. Gomeza, J., Ohno, K., Hulsmann, S., Armsen, W., Eulenburg, V., Richter, D. W., Laube, B., and Betz, H. (2003) *Neuron* **40,** 797–806
19. Dingledine, R., Kleckner, N. W., and McBain, C. J. (1990) *Adv. Exp. Med. Biol.* **268,** 17–26
20. Gabernet, L., Pauly-Evers, M., Schwerdel, C., Lentz, M., Bluethmann, H., Vogt, K., Alberati, D., Mohler, H., and Boison, D. (2005) *Neurosci. Lett.* **373,** 79–84
21. Tsai, G., Ralph-Williams, R. J., Martina, M., Bergeron, R., Berger-Sweeney, J., Dunham, K. S., Jiang, Z., Caine, S. B., and Coyle, J. T. (2004) *Proc. Natl. Acad. Sci. U. S. A.* **101,** 8485–8490
22. Ebihara, S., Yamamoto, T., Obata, K., and Yanagawa, Y. (2004) *Biochem. Biophys. Res. Commun.* **317,** 857–864
23. Fiser, A., and Sali, A. (2003) *Methods Enzymol.* **374,** 461–491
24. Giros, B., el Mestikawy, S., Godinot, N., Zheng, K., Han, H., Yang-Feng, T., and Caron, M. G. (1992) *Mol. Pharmacol.* **42,** 383–390
25. Hein, P., Frank, M., Hoffmann, C., Lohse, M. J., and Bunemann, M. (2005) *EMBO J.* **24,** 4106–4114
26. Dutertre, S., Nicke, A., and Lewis, R. J. (2005) *J. Biol. Chem.* **280,** 30460–30468
27. Eulenburg, V., Becker, K., Gomeza, J., Schmitt, B., Becker, C. M., and Betz, H. (2006) *Biochem. Biophys. Res. Commun.* **348,** 400–405
28. Schmid, J. A., and Sitte, H. H. (2003) *Curr. Opin. Oncol.* **15,** 55–64
29. Xia, Z., and Liu, Y. (2001) *Biophys. J.* **81,** 2395–2402
30. Seidel, S., Singer, E. A., Just, H., Farhan, H., Scholze, P., Kudlacek, O., Holy, M., Koppatz, K., Krivanek, P., Freissmuth, M., and Sitte, H. H. (2005) *Mol. Pharmacol.* **67,** 140–151
31. Sorkin, A., McClure, M., Huang, F., and Carter, R. (2000) *Curr. Biol.* **10,** 1395–1398
32. Korkhov, V. M., Holy, M., Freissmuth, M., and Sitte, H. H. (2006) *J. Biol. Chem.* **281,** 13439–13448
33. Nunez, E., and Aragon, C. (1994) *J. Biol. Chem.* **269,** 16920–16924

34. Fornes, A., Nunez, E., Aragon, C., and Lopez-Corcuera, B. (2004) *J. Biol. Chem.* **279,** 22934–22943
35. Armsen, W., Himmel, B., Betz, H., and Eulenburg, V. (2007) *Mol. Cell. Neurosci.* **36,** 369–380
36. Miranda, M., Sorkina, T., Grammatopoulos, T. N., Zawada, W. M., and Sorkin, A. (2004) *J. Biol. Chem.* **279,** 30760–30770
37. Just, H., Sitte, H. H., Schmid, J. A., Freissmuth, M., and Kudlacek, O. (2004) *J. Biol. Chem.* **279,** 6650–6657
38. Torres, G. E., Carneiro, A., Seamans, K., Fiorentini, C., Sweeney, A., Yao, W. D., and Caron, M. G. (2003) *J. Biol. Chem.* **278,** 2731–2739
39. Farhan, H., Reiterer, V., Korkhov, V. M., Schmid, J. A., Freissmuth, M., and Sitte, H. H. (2007) *J. Biol. Chem.* **282,** 7679–7689
40. Aragon, C., and Lopez-Corcuera, B. (1998) *Methods Enzymol.* **296,** 3–17
41. Cai, G., Salonikidis, P. S., Fei, J., Schwarz, W., Schulein, R., Reutter, W., and Fan, H. (2005) *FEBS J.* **272,** 1625–1638
42. Martinez-Maza, R., Poyatos, I., Lopez-Corcuera, B., Nunez, E., Gimenez, C., Zafra, F., and Aragon, C. (2001) *J. Biol. Chem.* **276,** 2168–2173
43. Fernandez-Sanchez, E., Diez-Guerra, F. J., Cubelos, B., Gimenez, C., and Zafra, F. (2007) *Biochem. J.* **409,** 669–681
44. Hahn, M. K., Robertson, D., and Blakely, R. D. (2003) *J. Neurosci.* **23,** 4470–4478
45. Rees, M. I., Harvey, K., Pearce, B. R., Chung, S. K., Duguid, I. C., Thomas, P., Beatty, S., Graham, G. E., Armstrong, L., Shiang, R., Abbott, K. J., Zuberi, S. M., Stephenson, J. B., Owen, M. J., Tijssen, M. A., van den Maagdenberg, A. M., Smart, T. G., Supplisson, S., and Harvey, R. J. (2006) *Nat. Genet.* **38,** 801–806